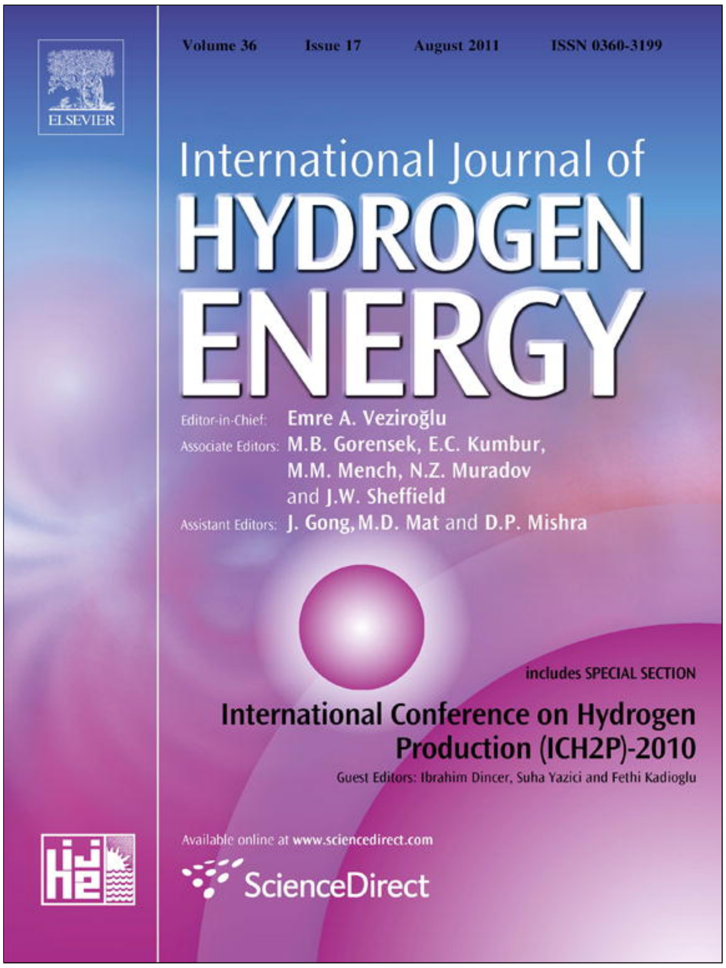
Volume 36 Issue 17 August 2011 ISSN 0360-3199
ELSEVIER
International Journal of
HYDROGEN
ENERGY
Editor-in-Chief: Emre A. Veziroğlu
Associate Editors: M.B. Gorensek, E.C. Kumbur, M.M. Mench, N.Z. Muradov and J.W. Sheffield
Assistant Editors: J. Gong, M.D. Mat and D.P. Mishra
includes SPECIAL SECTION
International Conference on Hydrogen Production (ICH2P)-2010
Guest Editors: Ibrahim Dincer, Suha Yazici and Fethi Kadioglu
Available online at www.sciencedirect.com
ScienceDirect

INTERNATIONAL JOURNAL OF HYDROGEN ENERGY 36 (2011) 11085–11092

Available at www.sciencedirect.com

journal homepage: www.elsevier.com/locate/he

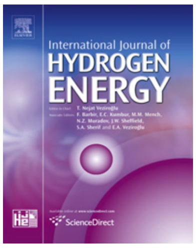

Atomic layer deposition assisted Pt-SnO_2 hybrid catalysts on nitrogen-doped CNTs with enhanced electrocatalytic activities for low temperature fuel cells

Yougui Chen [a], *Jiajun Wang* [a], *Xiangbo Meng* [a], *Yu Zhong* [a], *Ruying Li* [a], *Xueliang Sun* [a,*], *Siyu Ye* [b], *Shanna Knights* [b]

[a] *Department of Mechanical and Materials Engineering, University of Western Ontario, London, ON N6A 5B9, Canada*
[b] *Ballard Power Systems Inc., 9000 Glenlyon Parkway, Burnaby, BC V5J 5J8, Canada*

ARTICLE INFO

Article history:
Received 19 January 2011
Received in revised form
23 May 2011
Accepted 24 May 2011
Available online 23 June 2011

Keywords:
Pt
SnO_2
Nitrogen-doped carbon nanotube
Fuel cell
Atomic layer deposition

ABSTRACT

Nitrogen doped carbon nanotubes (CN_x) of a high nitrogen concentration were synthesized directly on carbon paper as the skeleton of a 3D composite electrode. Ultra-fine SnO_2 nanoparticles about 1.5 nm were deposited on CN_x with atomic layer deposition (ALD) technique. Pt nanoparticles from 1.5 to 4 nm were deposited on CN_x/carbon paper and SnO_2/CN_x/carbon paper with ethylene glycol reduction method. Three dimensional Pt/CN_x/carbon paper and Pt-SnO_2/CN_x/carbon paper composite electrodes were obtained, respectively. They were characterized over oxygen reduction reaction (ORR) and methanol oxidation reaction (MOR) for low temperature fuel cells. With similar sizes of Pt nanoparticles, the electrochemical surface area (ECSA) of Pt-SnO_2/CN_x/carbon paper is larger than that of Pt/CN_x/carbon paper. Pre-deposited SnO_2 nanoparticles promote the electrocatalytic activity of Pt toward ORR, carbon monoxide (CO) stripping and MOR. The underlying mechanisms for the enhanced activities are discussed.

1. Introduction

Fuel cell is a promising choice for clean energy because of its eco-friendly system, high energy conversion efficiency and high power density. Low temperature fuel cells, involved with proton-exchange membranes as the solid electrolyte, draw a great deal of attentions because of its low operating temperature and wide applications including automobiles, on-site power generation, back-up power, fork-lifts, and portable electronic devices. Although hydrogen is an ideal fuel for low temperature fuel cells (proton-exchange membrane fuel cell, PEMFC), challenges remain in the production and storage of H_2. To bypass these disadvantages, the direct methanol fuel cell (DMFC) has been developed with aqueous methanol as the fuel. Methanol, as a liquid at room temperature, makes storage and transport much easier. Methanol also contains a high energy density (6 kWh kg^{-1}), involving 6 electrons in the complete oxidation to CO_2 [1].

Despite considerable advances in recent years, technical and economical barriers still exist, hindering the widespread application of low temperature fuel cells. Both PEMFC and DMFC are limited by the sluggish kinetics of oxygen reduction reaction (ORR) at the cathode. The cell voltage is therefore lowered to ~0.4–0.7 V at practical current densities compared to the thermodynamic voltage of 1.23 V [2]. This drawback results in the reduced efficiency of the energy conversion in low temperature fuel cells. The slow kinetics of ORR requires a high loading of Pt at the cathode to reduce oxygen

---

[*] *Corresponding author*. Tel.: +1 519 6612111x87759; fax: +1 519 6613020.
E-mail address: xsun@eng.uwo.ca (X. Sun).

0360-3199/$ – see front matter Copyright © 2011, Hydrogen Energy Publications, LLC. Published by Elsevier Ltd. All rights reserved.
doi:10.1016/j.ijhydene.2011.05.156

effectively. But the high price and low reserve of Pt prohibit the commercialization of low temperature fuel cells.

Different from the PEMFC, the DMFC is also limited by the poor electrocatalytic activity toward methanol oxidation reaction (MOR) at the anode, which accounts for a further voltage loss of more than 0.3 V [2]. The slow kinetics of MOR is mostly due to the surface poisoning on Pt by reaction intermediates, mainly CO, formed by dehydrogenation of methanol. Endeavors to mitigate the poisoning of Pt have been focusing on the addition of co-catalysts, particularly Ru [2,3]. However, Ru is also an expensive noble metal. Further reduction of the cost and improvement of anodic catalytic performance for DMFC are still the key issues.

Besides alloying Pt with other transition metals, the addition of metal oxides is also investigated to enhance the electrocatalytic activity for MOR and ORR. Many studies have demonstrated that the addition of metal oxides to Pt results in more active electrocatalysts for both ORR and MOR. It was reported that TiO_2 enhanced both the activity and durability of Pt for the ORR [4] and MOR [5,6]. Sun *et al.* showed that Pt/WO_3/C was more active for ORR in sulfuric acid than Pt/C catalysts [7]. Jafri *et al.* demonstrated that the electrocatalytic activity of Au toward ORR can be improved by adding MnO_2 or ZnO [8]. Sasaki *et al.* found that niobium oxides improved the activity of Pt over ORR [9]. Xu *et al.* studied the positive effect of CeO_2 on Pt/C toward alcohol electrooxidation [10,11]. The enhanced activities were attributed to the high dispersion of Pt nanoparticles, electronic effect and/or bifunctional mechanism of metal oxides.

Among various metal oxides, SnO_2 is vigorously researched because of its high electronic conductivity, and stability in low temperature fuel cell working conditions [12]. Previously, we reported SnO_2 nanowires as catalyst support, which enhanced the activity for ORR and MOR [13,14]. As a co-catalyst, SnO_2 was also found to enhance the activity of Au toward ORR [15–17]. The activity of Pt over MOR [1,18], ethanol oxidation [19] and ORR [20] was also enhanced by the addition of SnO_2. This promotional role of SnO_2 in activity may be further improved if smaller sized SnO_2 can be obtained and thus higher specific surface area is offered. Atomic layer deposition (ALD), based on sequential and self-limiting surface reactions, provides a powerful method for the coating of ultra-fine metal oxides.

Our previous reports indicated that pristine nitrogen-doped carbon nanotubes (CN_x) are active for nanoparticles deposition on the surface [21,22]. Compared with carbon nanotubes (CNTs), Pt deposited on CN_x shows higher electrocatalytic activity and durability. In this work, combining the advantage of ALD technique and the intrinsic merits of CN_x, SnO_2 nanoparticles were deposited on CN_x by atomic layer deposition (ALD) [23], and investigated as the co-catalyst of Pt for low temperature fuel cells.

2. Experimental

2.1. Synthesis of CN_x

CN_x were directly synthesized on a commercial carbon paper (denoted as CN_x/carbon paper) as reported previously [24]. Briefly, carbon paper sputtered with a 30 nm Al buffer layer and then a 5 nm Fe catalyst film was placed at the heating center and 3 g melamine was placed at the upstream part of the quartz tube in a horizontal furnace. Melamine acted both as the carbon and nitrogen precursors to yield CN_x at 800 °C. The nitrogen concentration is 10.4 at. % based on the X-ray photoelectron spectroscopy (XPS) measurement [24].

2.2. SnO_2 deposition with atomic layer deposition

Polycrystalline SnO_2 was deposited on the CN_x/carbon paper (SnO_2/CN_x/carbon paper) by atomic layer deposition (ALD) as described elsewhere [25]. $SnCl_4$ and deionized water as precursors were introduced into the reactor in an alternating manner. Nitrogen (20 sccm) was applied as the carrier gas, and reactor was kept at the pressure of 0.4 Torr. The reaction was set at 400 °C for 50 cycles.

2.3. Pt nanoparticles deposition

Pt nanoparticles were deposited on the SnO_2/CN_x/carbon paper electrode by ethylene glycol reduction method. Briefly, the SnO_2/CN_x/carbon paper electrode was refluxed at 160 °C for 3 h in 50 ml ethylene glycol solution containing 0.2 mM $H_2PtCl_6.6H_2O$. Then the electrode was dried at 60 °C overnight in a vacuum oven. The obtained composite electrode is denoted as Pt-SnO_2/CN_x/carbon paper. Pt nanoparticles were also deposited on CN_x/carbon paper, denoted as Pt/CN_x/carbon paper, as a baseline for comparison.

2.4. Physical characterizations

The morphology of CN_x was characterized with field emission scanning electron microscopy (SEM, Hitachi S-4800, 5 kV). The structure of CN_x and dispersion of SnO_2 and Pt nanoparticles were investigated with transmission electron microscopy (TEM, Philips CM10, 80 kV). The energy dispersive spectroscopy (EDS) was taken with the above SEM at 20 kV. The Pt loading was tested with inductive coupled plasma-optical emission spectroscopy (ICP-OES, Varian Vista-Pro).

2.5. Electrochemical characterizations

The electrochemical characterizations were conducted with an Autolab potentiostat/galvanostat (Model PGSTAT-30, Ecochemie, Brinkman Instruments). Pt wire and Ag/AgCl (3 M NaCl) was served as the counter and reference electrode respectively. All potentials in this work are referred to the standard hydrogen electrode (SHE). Cyclic voltammograms were recorded in N_2 saturated 0.5 M H_2SO_4. The electrocatalytic activity for ORR was evaluated in O_2 saturated 0.5 M H_2SO_4 with linear scanning voltammetry at a scan rate of 50 mV s^{-1}. The catalytic activity toward MOR was investigated in 0.5 M H_2SO_4 with 1 M methanol. Since CO is an important reaction intermediate of the methanol oxidation, the CO stripping was also conducted. CO (99.5%) was purged for 30 min to achieve saturation. A monolayer of CO absorbed on Pt surface was obtained by purging N_2 for 30 min while with the working electrode polarized at 0.05 V. Voltammetry was applied for CO strip at last. All the electrochemical characterizations were conduced at room temperature.

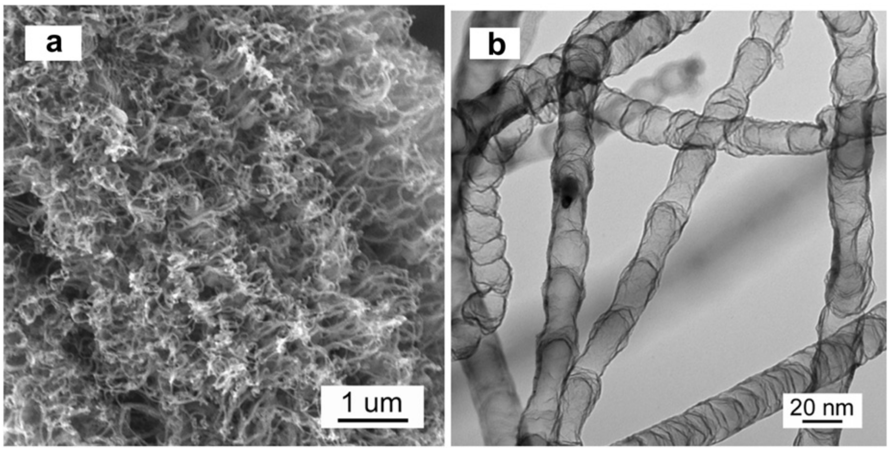

Fig. 1 – SEM (a) and TEM (b) images of CN_x synthesized on carbon paper.

3. Results and discussion

3.1. Physical characterizations

Fig. 1 shows the SEM (a) and TEM (b) images of CN_x grown on carbon paper. SEM image (Fig.1a) indicates the general morphology. CN_x are vertically extended from carbon fiber with high density and uniform dispersion. TEM image (Fig. 1b) shows the further information of the structure of CN_x. All the CN_x exhibit a bamboo-like structure, which is typical for CN_x [26]. The tube is divided into hollow sections separated by graphite layers. The CN_x shows a uniform distribution in tube diameters from 20 to 30 nm.

SnO_2 nanoparticles are uniformly dispersed on the surface of CN_x by ALD, as presented in Fig. 2a. In contrast to the clean surface of CN_x shown in Fig. 1b, ultra-fine SnO_2 nanoparticles around 1.5 nm can be clearly observed on the surface of CN_x. EDS spectra of CN_x and SnO_2/CN_x are compared in Fig. 2b. The strongest peak, carbon, comes from the CN_x and the carbon paper substrate. Al and Fe peaks can be ascribed to the Al buffer layer and Fe catalyst film on carbon paper for the synthesis of CN_x [24]. SnO_2/CN_x shows two additional peaks of Sn and O resulted from the deposited SnO_2 nanoparticles, which is in good agreement with the TEM observation in Fig. 2a.

To compare the two substrates as catalyst supports, Pt nanoparticles are deposited on both CN_x/carbon paper and SnO_2/CN_x/carbon paper with ethylene glycol reduction method with the same procedure. Fig. 3 exhibits the TEM images and distribution histograms based on the counting of 200 Pt nanoparticles on the two supports. In both cases, Pt nanoparticles dispersed uniformly on the support with a narrow size distribution from 1.5 to 4 nm. The mean size of Pt on Pt/CNx/carbon paper and Pt-SnO_2/CNx/carbon paper is 2.5 and 2.6 nm respectively. This suggests that the SnO_2 pre-deposited on CN_x has no remarkable influence on the distribution of the subsequent Pt nanoparticles.

3.2. Electrochemical characterizations

It is introduced above that metal oxides can improve the catalytic activities of Pt toward ORR and MOR [4–20]. Hence, electrochemical characterizations were applied to evaluate the electrocatalytic activities of the two composite electrodes. The cyclic voltammograms of both Pt/CN_x/carbon paper and

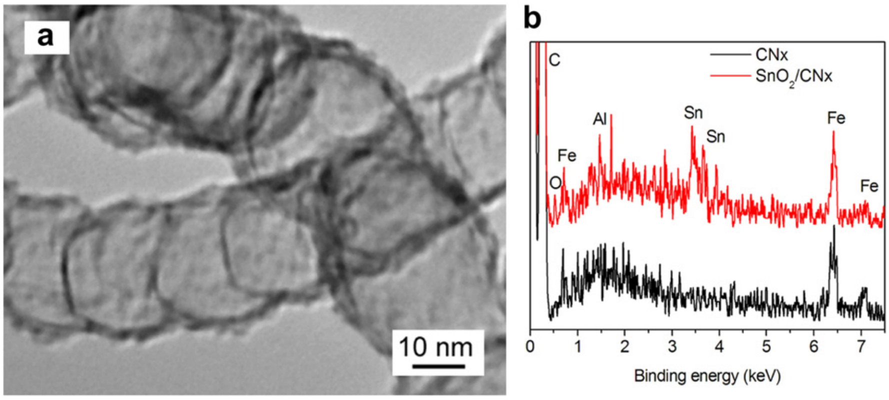

Fig. 2 – (a) TEM image of SnO_2 nanoparticles deposited on CN_x by ALD for 50 cycles and (b) the EDX spectra of CN_x and SnO_2/CN_x.

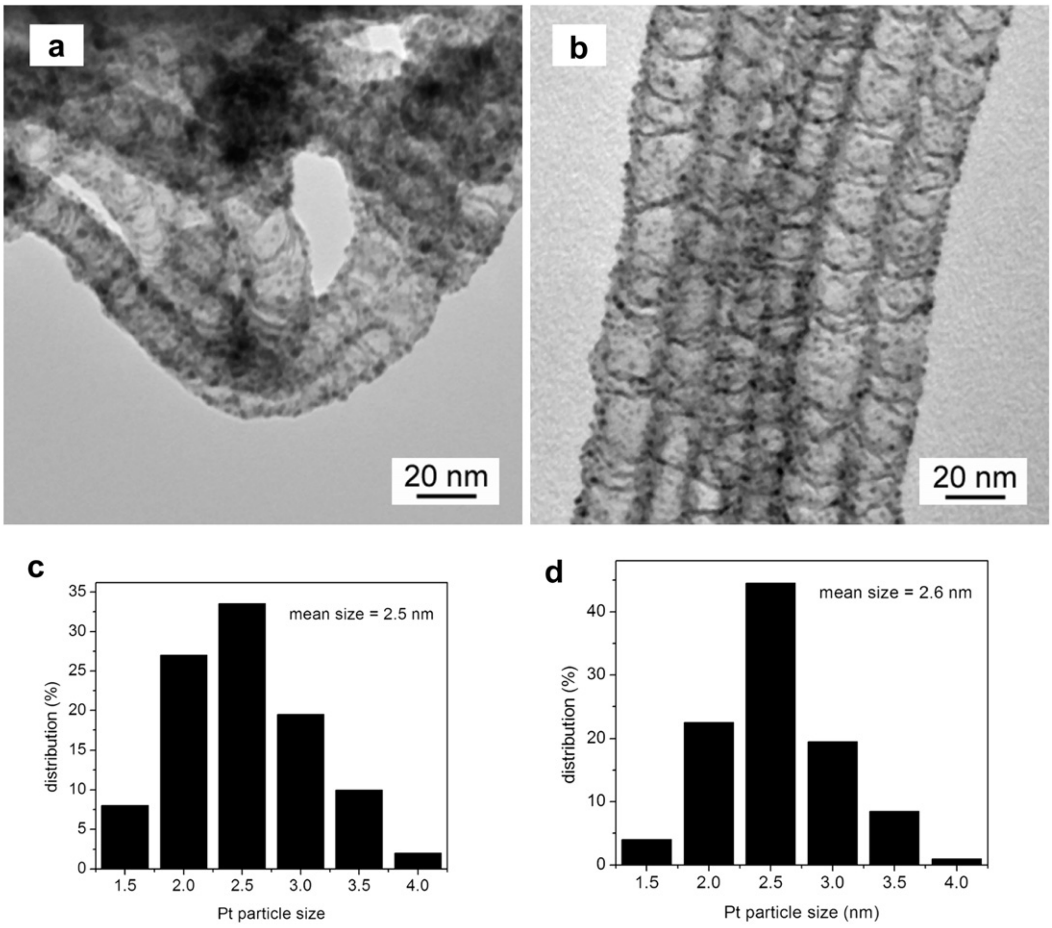

Fig. 3 – TEM images and Pt particle size distributions of Pt/CN_x (a, c) and Pt-SnO_2/CN_x (b, d).

Pt-SnO_2/CN_x/carbon paper are presented in Fig. 4. Cyclic voltammograms of typical Pt features are obtained, with H_2 adsorption/desorption regions and Pt oxidation/reduction peaks. The electrochemical surface area (ECSA) of Pt is calculated from the charges of H_2 adsorption/desorption peaks, assuming a surface density of 1.3×10^{15} atom/cm^2 for polycrystalline Pt [27].

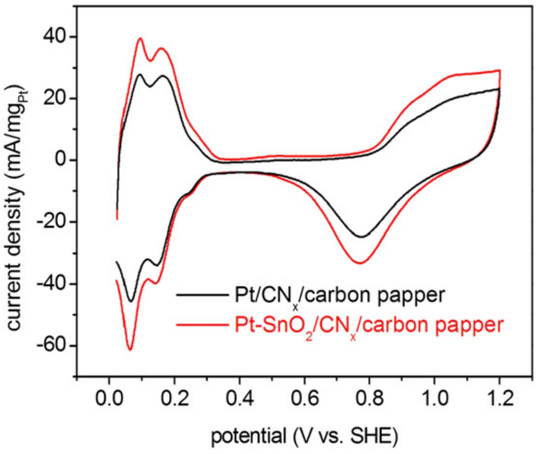

Fig. 4 – Cyclic voltammograms of Pt/CN_x/carbon paper and Pt-SnO_2/CN_x/carbon paper electrodes in 0.5 M H_2SO_4 solution at 50 mV s^{-1}.

$$\mathrm{ECSA} = \frac{Q_H}{Q_{ref}\, m_{Pt}} \tag{E1}$$

Where Q_H is the average charge of the hydrogen adsorption and desorption from the cyclic voltammogram; Q_{ref} (0.21 mC cm^{-2}) is the charge required to oxidize a monolayer of H_2 on a smooth Pt surface; and m_{Pt} is the Pt loading on CN_x/carbon paper or SnO_2/CN_x/carbon paper from ICP-OES tests, which is 0.085 and 0.077 mg respectively. Pt-SnO_2/CN_x shows an ECSA of 72.6 m^2 $g^{-1}{}_{Pt}$, whereas the ECSA of Pt/CN_x is 53.3 m^2 $g^{-1}{}_{Pt}$. That is, the ECSA of Pt-SnO_2/CN_x is 1.36 times of that of Pt/CN_x. The discrepancy in ECSA may be explained by the slight size difference of Pt nanoparticles and/or Pt-metal oxide interaction. The positive effect of SnO_2 on the ECSA of Pt is in good agreement with other reports [28,29], which attribute it to the OH removal on Pt by SnO_2. The OH generates on the surface of SnO_2 first and prohibits the OH formation on Pt surface. It is well recognized that the electrocatalysis takes place at the surface. The larger ECSA, the higher electrocatalytic activity it has. The results above suggest that predeposited SnO_2 improves the Pt utilization and results in a better catalyst than Pt/CN_x/carbon paper.

The electrocatalytic activities over ORR of the two catalysts are compared in Fig. 5 by linear scanning voltammetry at a scan rate of 50 mV s^{-1}. The electrocatalytic activities of the two composite electrodes are summarized in Table 1. Pt-SnO_2/

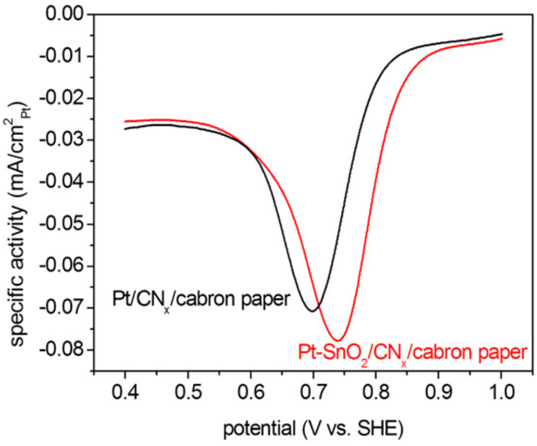

Fig. 5 – ORR activities of Pt/CN$_x$/carbon paper and Pt-SnO$_2$/CN$_x$/carbon paper in O$_2$ saturated 0.5 M H$_2$SO$_4$ solution at 50 mV s^{-1}.

CN$_x$/carbon paper shows a higher peak potential than Pt/CN$_x$/carbon paper. The peak potential of Pt-SnO$_2$/CN$_x$/carbon paper is 0.740 V, while that of Pt/CN$_x$/carbon paper is 0.698 V, suggesting that Pt-SnO$_2$/CN$_x$/carbon paper exhibits a 42 mV positive shift of the peak potential compared with Pt/CN$_x$/carbon paper toward ORR. At 0.85 V, the mass activity on Pt-SnO$_2$/CN$_x$/carbon paper is 10.836 mA mg$^{-1}_{Pt}$, while it is 4.587 mA mg$^{-1}_{Pt}$ on Pt/CN$_x$/carbon paper; and the specific activity on Pt-SnO$_2$/CN$_x$/carbon paper and Pt/CN$_x$/carbon paper is 0.015 and 0.009 mA cm$^{-2}_{Pt}$, respectively. The mass activity on Pt-SnO$_2$/CN$_x$/carbon paper is 2.36 times of that on Pt/CN$_x$/carbon paper; and the specific activity on Pt-SnO$_2$/CN$_x$/carbon paper is 1.67 times of that on Pt/CN$_x$/carbon paper at 0.85 V. The larger specific activity, mass activity and more positive peak potential propose that Pt-SnO$_2$/CN$_x$/carbon paper has a higher intrinsic electrocatalytic activity than Pt/CN$_x$/carbon paper. In other words, pre-deposited SnO$_2$ nanoparticles can promote the catalytic activity of Pt toward ORR. The possibility of PtSn alloy catalyst can be excluded because SnO$_2$ cannot be reduced in ethylene glycol at temperatures lower than 200 °C [30]. The XPS results by Ignaszak *et al.* also confirm the absence of metallic Sn after the reduction by ethylene glycol [31]. The mechanism for the enhanced electrocatalytic activity is open to discussion. First of all, SnO$_2$ itself is active for ORR in acid medium. Liu *et al.* recently reported that tin oxide films by sputtering methods displayed a certain activity for ORR [32]. Secondly, the lateral repulsion from the OH or other oxygen species on the SnO$_2$ surface prevents the generation of oxygen species on the adjacent Pt and so makes it a clean metallic surface for ORR. It is well recognized that the inhibition effect of OH adsorbed on Pt is a major cause of the large overpotential for ORR [33]. Thirdly, the electronic interaction between Pt and metal oxides can also improve the electrocatalytic activity of Pt, as discussed in the cases of Pt-niobium oxide [9] and Au-tin oxide [15,16]. The interaction can modify the Pt electronic structure, which is sensitive toward ORR, as shown by density functional theory calculations [34]. Finally, a bifunctional mechanism is proposed to interpret the enhanced electrocatalytic activity with SnO$_2$. The rate-determining step of ORR is the addition of the first electron to O$_2$ [35]. The chemisorbed O$_2^-$ on SnO$_2$ can transfer to Pt for future reduction [16]. All the aforementioned factors can contribute to the enhanced intrinsic electrocatalytic activity of Pt-SnO$_2$/CN$_x$/carbon paper toward ORR, in comparison with Pt/CN$_x$/carbon paper.

CO, a critical intermediate of MOR, can poison Pt catalysts. CO stripping was conducted to compare the activity over CO electrochemical oxidation on the two electrodes, as presented in Fig. 6a. Pt/CN$_x$/carbon paper exhibits a single sharp peak centered at 0.768 V. On the Pt-SnO$_2$/CN$_x$/carbon paper, the CO oxidation peak is significantly broadened, with a strong peak at 0.671 V and a small shoulder peak around 0.728 V. The CO oxidation peak potential shifts negatively 97 mV on Pt-SnO$_2$/CN$_x$/carbon paper compared with Pt/CN$_x$/carbon paper. Such a negative shift of CO stripping peak is also observed by others [28,36]. It indicates that Pt-SnO$_2$/CN$_x$/carbon paper is more effective than Pt/CN$_x$/carbon paper for electrooxidation of the adsorbed CO. In addition, the broad peak with a shoulder indicates that there are different active sites for CO electrooxidation on Pt-SnO$_2$/CN$_x$/carbon paper electrode. It is well accepted that hydroxyl (OH) is required to oxidize the absorbed CO to CO$_2$ [2], as presented in the following reactions.

$$\mathrm{Pt} + \mathrm{H_2O} \rightarrow \mathrm{Pt-OH} + \mathrm{H^+} + \mathrm{e^-} \tag{R 1a}$$

$$\mathrm{SnO_2} + \mathrm{H_2O} \rightarrow \mathrm{SnO_2-OH} + \mathrm{H^+} + \mathrm{e^-} \tag{R 1b}$$

$$\mathrm{Pt-CO} + \mathrm{Pt-OH} \rightarrow 2\mathrm{Pt} + \mathrm{CO_2} + \mathrm{H^+} + \mathrm{e^-} \tag{R 2a}$$

$$\mathrm{Pt-CO} + \mathrm{SnO_2-OH} \rightarrow \mathrm{Pt} + \mathrm{SnO_2} + \mathrm{CO_2} + \mathrm{H^+} + \mathrm{e^-} \tag{R 2b}$$

OH can be formed on the surface of SnO$_2$ (R 1b) at a much lower potential than that on Pt (R 1a) [36,37]. On Pt/CN$_x$/carbon paper, the absorbed CO is oxidized only by consuming the OH on Pt surface (R 2a) and result in a single peak at high

Table 1 – Summary of the electrocatalytic activities toward ORR and MOR on Pt-SnO$_2$/CN$_x$/carbon paper and Pt/CN$_x$/carbon paper composite electrodes.

Electrodes	ORR activity			MOR activity		
	Peak potential (V)	Specific activity @0.85 V (mA/cm$^2_{Pt}$)	Mass activity @0.85 V (mA/mg$_{Pt}$)	Onset potential (V)	Specific activity @0.65 V (mA/cm$^2_{Pt}$)	Mass activity @0.65 V (mA/mg$_{Pt}$)
Pt/CN$_x$/carbon paper	0.740	0.009	4.587	0.588	0.051	23.2
Pt-SnO$_2$/CN$_x$/carbon paper	0.698	0.015	10.836	0.536	0.150	95.7

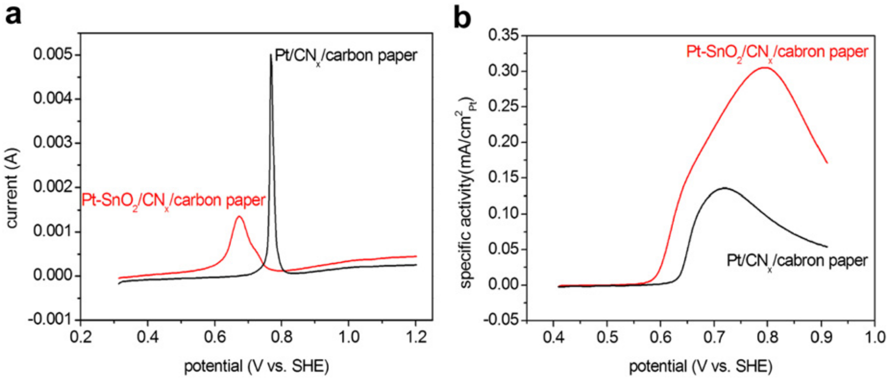

Fig. 6 – The comparison of (a) CO stripping in CO saturated 0.5 M H_2SO_4 and (b) methanol oxidation in 0.5 M H_2SO_4 with 1 M methanol, on Pt/CN_x/carbon paper and Pt-SnO_2/CN_x/carbon paper composite electrodes, respectively, with linear scan voltammetry at 1 mV s^{-1}.

potential, as indicated in Fig. 6a. On Pt-SnO_2/CN_x/carbon paper, on the other hand, the absorbed CO can be oxidized by either consuming the OH on Pt or SnO_2 through a bifunctional mechanism (R 2b) [38,39]. The electrooxidation of the CO absorbed on Pt adjacent to SnO_2 contributes to the main peak at a much lower potential compared with Pt/CN_x/carbon paper. Whereas, the diffusion of hydroxyl on metal oxide surface is slow [38]. On Pt apart from SnO_2, CO is oxidized by combining the hydroxyl diffused from SnO_2 or formed on Pt surface, which contributes to the shoulder peak positive to the main peak. Therefore, the pre-deposited SnO_2 can promote the electrooxidation of adsorbed CO on Pt. This suggests that Pt-SnO_2/CN_x/carbon paper is a better catalyst than Pt/CN_x/carbon paper for MOR, which is discussed below.

The electrocatalytic activities over MOR on Pt-SnO_2/CN_x/carbon paper and Pt/CN_x/carbon paper are compared in Fig. 6b. In the slow linear scanning voltammograms, Pt-SnO_2/CN_x/carbon paper shows a lower onset potential and a higher specific current at the same potential than Pt/CN_x/carbon paper. The onset potential of MOR on Pt-SnO_2/CN_x/carbon paper is 0.536 V, 52 mV more negative than 0.588 V, the onset potential on Pt/CN_x/carbon paper. At 0.65 V, the mass activity on Pt-SnO_2/CN_x/carbon paper is 95.7 mA/mg_{Pt}, while it is 23.2 mA/mg_{Pt} on Pt/CN_x/carbon paper; and the specific activity on Pt-SnO_2/CN_x/carbon paper is 0.150 mA/cm^2_{Pt}, while it is 0.051 mA/cm^2_{Pt} on Pt/CN_x/carbon paper respectively (as summarized in Table 1). The mass activity on Pt-SnO_2/CN_x/carbon paper is 4.12 times of that on Pt/CN_x/carbon paper; and the specific activity on Pt-SnO_2/CN_x/carbon paper is 2.94 times of that on Pt/CN_x/carbon paper at 0.85 V. Therefore, the electrocatalytic activity toward MOR on Pt is enhanced with the pre-deposited SnO_2 nanoparticles. This can be interpreted by the well-known bifunctional mechanism similar to PtRu catalysts [2,3]. The electrooxidation of methanol starts with the dehydrogenation, leading to CO as the intermediate strongly bonded to Pt surface. As discussed above, OH is needed to oxidize CO to CO_2. Since OH can be formed on SnO_2 (R 1b described above) at a lower potential than on Pt [37,38], a negative shift of the onset potential can be observed on Pt-SnO_2/CN_x/carbon paper compared with Pt/CN_x/carbon paper. In addition, the strong interaction [40] between Pt and SnO_2 may also be responsible for the enhanced activity toward MOR.

4. Conclusions

CN_x with a nitrogen concentration of 10.4 at.% have been synthesized directly on carbon paper with a high density and uniform distribution in tube diameters from 20 to 30 nm. With ALD, polycrystalline SnO_2 nanoparticles about 1.5 nm were deposited on CNx. Pt nanoparticles from 1.5 to 4 nm were deposited on CNx/carbon paper and SnO_2/CN_x/carbon paper with ethylene glycol reduction method. Despite similar size of Pt nanoparticles, the ECSA of Pt-SnO_2/CN_x/carbon paper is 1.36 times that of Pt/CN_x/carbon paper. Pt-SnO_2/CN_x/carbon paper shows a 42 mV more positive peak potential, and larger specific and mass activity than Pt/CN_x/carbon paper toward ORR. Pt-SnO_2/CN_x/carbon paper exhibits a 97 mV negative shift of the peak potential than Pt/CN_x/carbon paper on CO stripping. Pt-SnO_2/CN_x/carbon paper also shows higher activity over MOR than Pt/CN_x/carbon paper in terms of 52 mV more negative onset potential, and larger specific and mass activity. In our ongoing project, we are continuing to explore ALD deposition for further controlling the size and structure of SnO_2 and other metal oxides as co-catalysts of Pt for fuel cells.

Acknowledgements

This research was supported by Natural Sciences and Engineering Research Council of Canada (NSERC), Ballard Power System Inc., Canada Research Chair (CRC) Program, Canada Foundation for Innovation (CFI), Ontario Research Fund (ORF), Ontario Early Researcher Award (ERA) and the University of Western Ontario. Mike Sun is acknowledged for his useful suggestions.

REFERENCES

[1] Salazar-Banda GR, Suffredini HB, Avaca LA, Machado SAS. Methanol and ethanol electro-oxidation on Pt–SnO_2 and Pt–Ta_2O_5 sol–gel-modified boron-doped diamond surfaces. Mater Chem Phys 2009;117:434–42.

[2] Hogarth MP, Ralph TR. Catalysis for low temperature fuel cells PART III: challenges for the direct methanol fuel cell. Platinum Metals Rev 2002;46:146–64.

[3] Liu H, Song C, Zhang L, Zhang J, Wang H, Wilkinson DP. A review of anode catalysis in the direct methanol fuel cell. J Power Sources 2006;155:95–110.

[4] George PP, Pol VG, Gedanken A, Gabashvili A, Cai M, Mance AM, et al. Selective coating of anatase and rutile TiO_2 on carbon via ultrasound irradiation: mitigating fuel cell catalyst degradation. J Fuel Cell Sci Tech 2008;5: 041012–20.

[5] Zhang H, Zhou W, Du Y, Yang P, Wang C, Xu J. Enhanced electrocatalytic performance for methanol oxidation on Pt–TiO_2/ITO electrode under UV illumination. Int J Hydrogen Energy 2010;35:13290–7.

[6] Xing L, Jia J, Wang Y, Zhang B, Dong S. Pt modified TiO_2 nanotubes electrode: preparation and electrocatalytic application for methanol oxidation. Int J Hydrogen Energy 2010;35:12169–73.

[7] Sun Z, Chiu HC, Tseung ACC. Oxygen reduction on Teflon bonded Pt/WO_3/C electrode in sulfuric acid. Electrochem Solid-State Lett 2001;4:E9–12.

[8] Jafri RI, Sujatha N, Tajalakshmi N, Ramaprabhu S. Au–MnO_2/MWNT and Au–ZnO/MWNT as oxygen reduction reaction electrocatalyst for polymer electrolyte membrane fuel cell. Int J Hydrogen Energy 2009;34: 6367–71.

[9] Sasaki K, Zhang L, Adzic RR. Niobium oxide-supported platinum ultra-low amount electrocatalysts for oxygen reduction. Phys Chem Chem Phys 2008;10:159–67.

[10] Xu C, Shen PK. Electrochamical oxidation of ethanol on Pt-CeO_2/C catalysts. J Power Sources 2005;142:27–9.

[11] Xu C, Zeng R, Shen PK, Wei Z. Synergistic effect of CeO_2 modified Pt/C catalysts on the alcohols oxidation. Electrochim Acta 2005;51:1031–5.

[12] Masao A, Noda S, Takasaki E, Ito K, Sasaki K. Carbon-free Pt electrocatalysts supported on SnO_2 for polymer electrolyte fuel cells. Electrochem Solid-State Lett 2009;12: B119–22.

[13] Saha MS, Li R, Cai M, Sun X. High electrocatalytic activity of platinum nanoparticles on SnO_2 nanowire-based electrodes. Electrochem Solid-State Lett 2007;10:B130–3.

[14] Saha MS, Li R, Sun X. Composite of Pt–Ru supported SnO_2 nanowires grown on carbon paper for electrocatalytic oxidation of methanol. Electrochem Commun 2007;9: 2229–34.

[15] Gatewood DS, Ramaker DE, Sasaki K, Swider-Lyonsa KE. Support effects on water activation and oxygen reduction over Au–SnO_x electrocatalysts observed with X-ray absorption spectroscopy. J Electrochem Soc 2008;155: B834–42.

[16] Baker WS, Pietron JJ, Teliska ME, Bouwman PJ, Ramaker DE, Swider-Lyons KE. Enhanced oxygen reduction activity in acid by tin-oxide supported Au nanoparticle catalysts. J Electrochem Soc 2006;153:A1702–7.

[17] Moustafid TE, Cachet H, Tribollet B, Festy D. Modified transparent SnO_2 electrodes as efficient and stable cathodes for oxygen reduction. Electrochim Acta 2002;47: 1209–15.

[18] Yuan H, Guo D, Qiu X, Zhu W, Chen L. Influence of metal oxides on Pt catalysts for methanol electrooxidation using electrochemical impedance spectroscopy. J Power Sources 2009;188:8–13.

[19] Zhang X, Zhu H, Guo Z, Wei Y, Wang F. Design and preparation of CNT@SnO_2 core-shell composites with thin shell and its application for ethanol oxidation. Int J Hydrogen Energy 2010;35:8841–7.

[20] Parrondo J, Mijangos F, Rambabu B. Platinum/tin oxide/carbon cathode catalyst for high temperature PEM fuel cell. J Power Sources 2010;195:3977–83.

[21] Chen Y, Wang J, Liu H, Li R, Sun X, Ye S, et al. Enhanced stability of Pt electrocatalysts by nitrogen doping in CNTs for PEM fuel cells. Electrochem Commun 2009;11:2071–6.

[22] Saha MS, Li R, Sun X, Ye S. 3-D composite electrodes for high performance PEM fuel cells composed of Pt supported on nitrogen-doped carbon nanotubes grown on carbon paper. Electrochem Commun 2009;11:438–41.

[23] Knez M, Nielsch K, Niinistö L. Synthesis and surface engineering of complex nanostructures by atomic layer deposition. Adv Mater 2007;19:3425–38.

[24] Zhong Y, Jaidann M, Zhang Y, Zhang G, Liu H, Ionescu MI, et al. Synthesis of high nitrogen doping of carbon nanotubes and modeling the stabilization of filled DAATO@CNTs (10,10) for nanoenergetic materials. J Phys Chem Solids 2010;71: 134–9.

[25] Meng X, Zhong Y, Sun Y, Banis MN, Li R, Sun X. Nitrogen-doped carbon nanotubes coated by atomic layer deposited SnO_2 with controlled morphology and phase. Carbon 2011; 49:1133–44.

[26] Wang EG. Nitrogen-induced carbon nanobells and their properties. J Mater Res 2006;21:2767–73.

[27] Saha MS, Li R, Sun X. High loading and monodispersed Pt nanoparticles on multiwalled carbon nanotubes for high performance proton exchange membrane fuel cells. J Power Sources 2008;177:314–22.

[28] Jiang L, Colmenares L, Jusys Z, Sun GQ, Behm RJ. Ethanol electrooxidation on novel carbon supported Pt/SnO_x/C catalysts with varied Pt:Sn ratio. Electrochim Acta 2007;53: 377–89.

[29] Hsu RS, Higgins D, Chen Z. Tin-oxide-coated single-walled carbon nanotube bundles supporting platinum electrocatalyst for direct ethanol fuel cells. Nanotechnology 2010;21:165705–9.

[30] Larcher D, Patrice R. Preparation of metallic powders and alloys in polyol media: a thermodynamic approach. J Solid State Chem 2000;154:405–11.

[31] Ignaszak A, Teo C, Ye S, Gyenge E. Pt-SnO_2-Pd/C electrocatalyst with enhanced activity and durability for the oxygen reduction reaction at low Pt loading: the effect of carbon support type and activation. J Phys Chem C 2010;114: 16488–504.

[32] Liu Y, Ishihara A, Mitsushima S, Kamiya N, Ota K. Transition metal oxides as DMFC cathodes without platinum. J Electrochem Soc 2007;154:B664–9.

[33] Wang JX, Markovic NM, Adzic RR. Kinetic analysis of oxygen reduction on Pt(111) in acid solutions: intrinsic kinetic parameters and anion adsorption effects. J Phys Chem B 2004;104:4127–33.

[34] Stamenkovic V, Mun BS, Mayrhofer KJJ, Ross PN, Markovic N, Rossmeisl J, et al. Changing the activity of electrocatalysts for oxygen reduction by tuning the surface electronic structure. Angew Chem Int Ed 2006;45:2897–901.

[35] Blizanac BB, Lucas CA, Gallagher ME, Arenz M, Ross PN, Markovic NM. Anion adsorption, CO oxidation, and oxygen reduction reaction on a Au(100) surface: the pH effect. J Phys Chem B 2004;108:625–34.

[36] Lee KS, Park IS, Cho YH, Jung DS, Jung N, Park HY, et al. Electrocatalytic activity and stability of Pt supported on Sb-doped SnO_2 nanoparticles for direct alcohol fuel cells. J Catal 2008;258:143–52.

[37] Barretto CB, Parreira RLT, Goncalves RR, Azevedo DC, Huguenin F. Platinum nanoparticles embedded in layer-by-layer films from SnO_2/polyallylamine for ethanol electrooxidation. J Power Sources 2008;185:6–12.

[38] Yuan H, Guo D, Li X, Yuan L, Zhu W, Chen L, et al. The effect of CeO_2 on Pt/CeO_2/CNT catalyst for CO electrooxidation. Fuel Cells 2009;9:121–7.

[39] Arenz M, Stamenkovic V, Blizanac BB, Mayrhofer KJ, Markovic NM, Ross PN. Carbon-supported Pt–Sn electrocatalysts for the anodic oxidation of H_2, CO, and H_2/CO mixtures. Part II: the structure–activity relationship. J Catal 2005;232:402–10.

[40] Okanishi T, Matsui T, Takeguchi T, Kikuchi R, Eguchi K. Chemical interaction between Pt and SnO_2 and influence on adsorptive properties of carbon monoxide. Appl Catal A Gen 2006;298:181–7.